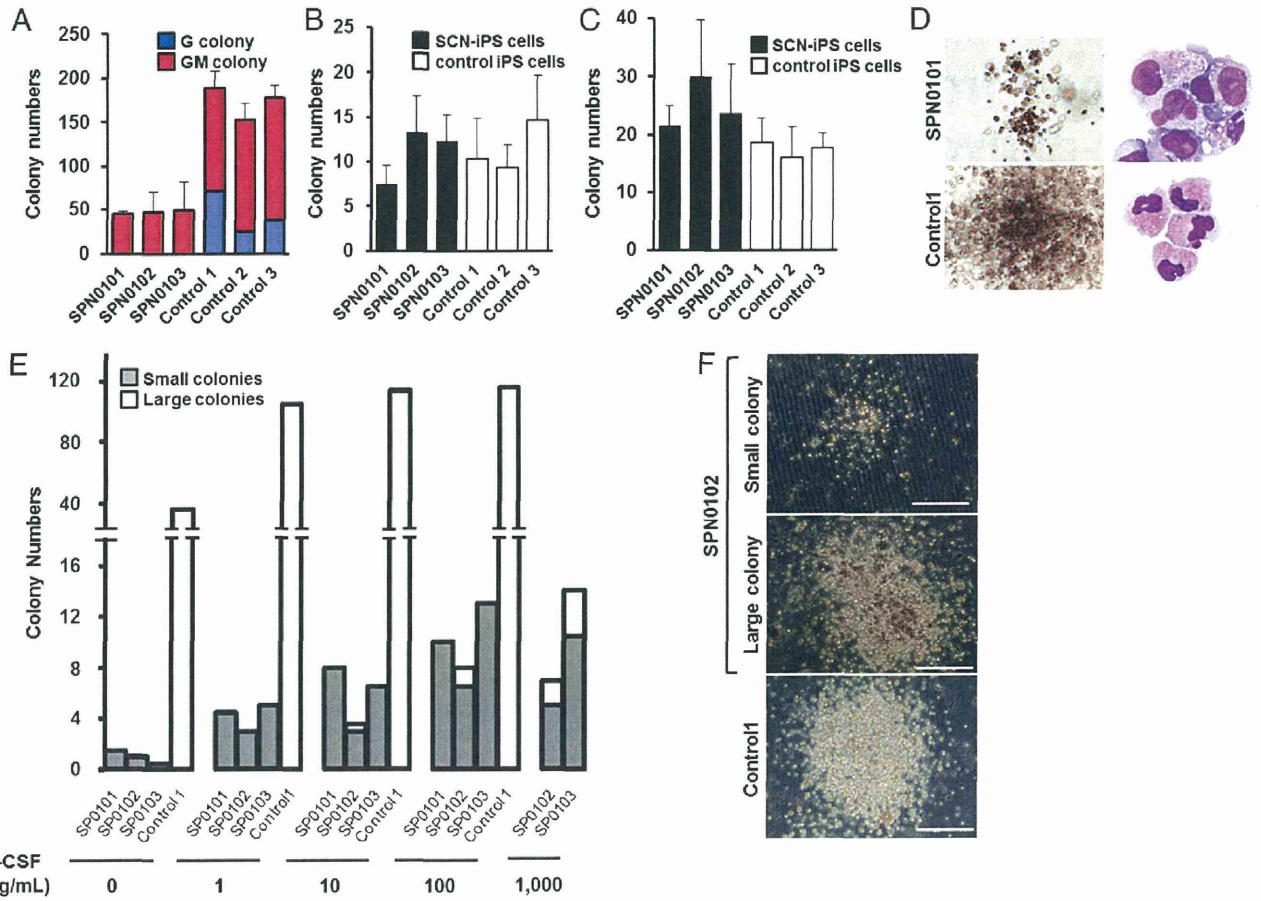

Fig. 1. Impaired neutrophil development from SCN-iPS cells. (*A–C*) A hematopoietic colony assay was performed by using 1×10^4 $CD34^+$ cells derived from three SCN-iPS cell clones (SPN0101, SPN0102, and SPN0103) and three control iPS cell clones (controls 1, 2, and 3) in the presence of a cytokine mixture. Colonies were sorted as myeloid (*A*), erythroid (*B*), and mixed-lineage (Mix) (*C*). Data are shown as mean ± SD. (*D*) Photographs of colonies (*Left*; 100×) and cells in a GM colony (*Right*; 400×; May–Grünwald–Giemsa staining). (*E*) A hematopoietic colony assay with dose escalation of G-CSF was performed by using 1×10^5 $CD34^+$ cells derived from SCN-iPS and control iPS cells. Filled and open bars indicate small colonies consisting of <100 cells and large colonies consisting of >100 cells, respectively. Data are shown as the average of three independent experiments. (*F*) Photographs of a small colony derived from SCN-iPS cells (*SPN0102*) in the presence of 10 ng/mL G-CSF, large colonies derived from SCN-iPS cells in the presence of 1,000 ng/mL G-CSF, and large colonies derived from control iPS cells (control 1) in the presence of 10 ng/mL G-CSF. (Scale bars, 200 μm.)

and *D*). In particular, only a few SCN-iPS cell-derived granulocyte (G) colonies—myeloid colonies consisting of only granulocytes—were detected (Fig. 1*A*). SCN-iPS cell-derived granulocyte–macrophage (GM) colonies—myeloid colonies consisting of macrophages/monocytes with/without granulocytes—contained a few immature myeloid cells in addition to macrophages/monocytes, whereas control iPS cell-derived GM colonies included a substantial number of mature, segmented, and band neutrophils (Fig. 1*D*).

We also found that Mix colonies derived from SCN-iPS cells, but not control iPS cells, contained immature myeloid cells and few mature neutrophils (Fig. S2 *C* and *D*). Next, we conducted a hematopoietic colony assay using various concentrations of G-CSF alone instead of the cytokine mixture to examine the G-CSF dose dependency of neutrophil differentiation from SCN-iPS and control iPS–$CD34^+$ cells. For all concentrations of G-CSF used (1–1,000 ng/mL), the SCN-iPS cell-derived myeloid colonies were significantly lower in number and smaller in size than the control iPS cell-derived myeloid colonies (Fig. 1*E*). Myeloid colony formation from control iPS cells reached a plateau at ~1–10 ng/mL G-CSF, whereas the number and size of those from SCN-iPS cells gradually increased with increasing concentrations of G-CSF. However, the values observed for SCN-iPS cells did not reach those for the control iPS cells, even at the highest dose of G-CSF used (1,000 ng/mL). Furthermore, large colonies consisting of >100 cells derived from SCN-iPS cells were only found with higher concentrations of G-CSF (Fig. 1*F*). Thus, granulopoiesis initiated from SCN-iPS cells was relatively insensitive to G-CSF, reflecting the inadequate in vivo response of neutrophils to G-CSF in SCN patients (14, 15). Therefore, these results support the applicability of the SCN-iPS cells established herein as a disease model for SCN.

To examine neutrophil development from SCN-iPS cells in more detail, SCN-iPS and control iPS–$CD34^+$ cells (1×10^4 cells each) were cocultured in suspension with AGM-S3 cells in the presence of neutrophil differentiation medium (*SI Materials and Methods*). The number of nonadherent cells derived from SCN-iPS–$CD34^+$ cells was lower than that from control iPS–$CD34^+$ cells on day 14 of culture (SCN-iPS cells, $9.77 \times 10^4 \pm 1.65 \times 10^4$ cells; control iPS cells, $52.48 \times 10^4 \pm 23.13 \times 10^4$ cells; $P < 0.05$) (Fig. 2*A*). The proportion of mature neutrophils among the nonadherent cells was also significantly lower for SCN-iPS cells relative to control iPS cells on day 14 (SPN-iPS cells, 15.53% ± 4.33%; control iPS cells, 71.285 ± 3.30%; $P < 0.05$) (Fig. 2 *B* and *C*), indicating that myeloid cells derived from SCN-iPS cells revealed the maturation arrest in the neutrophil development. We then examined a possibility that the maturation arrest in SCN-

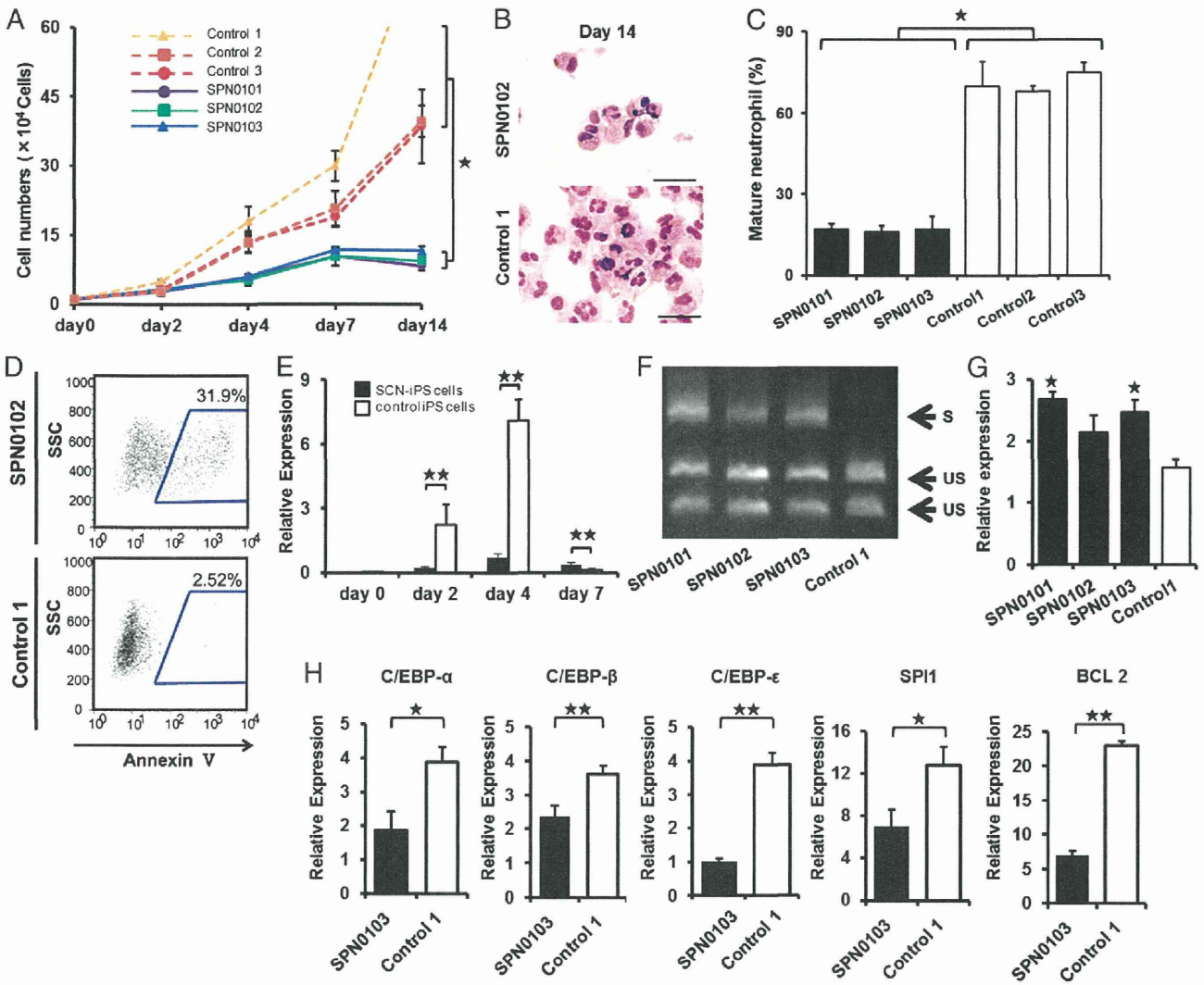

Fig. 2. Analysis of impaired neutrophil development from SCN-iPS cells. (*A*) Total number of nonadherent cells in the suspension culture of 1×10^4 $CD34^+$ cells derived from SCN-iPS and control iPS cells. Data are shown as mean ± SD. $^*P < 0.01$. (*B*) Photographs of nonadherent cells derived from SCN-iPS (SPN0103) and control iPS cells (control 1) on day 14 of culture (400×; May–Grünwald–Giemsa staining; scale bars, 50 μm.) (*C*) Filled and open bars show the proportion of mature neutrophils among the cells derived from SCN-iPS (filled bars) and control iPS (open bars) cells on day 14 of suspension culture. Data are shown as mean ± SD. $^*P < 0.05$. (*D*) Flow cytometric analysis of annexin V expression on cultured cells from SCN-iPS cells (SPN0102) or control iPS cells (control 1) on day 7. (*E*) Sequential qRT-PCR analysis of the relative expression of ELANE mRNA [ELANE/hypoxanthine–guanine phosphoribosyltransferase (HPRT) expression]. Data obtained from independent experiments using three SCN-iPS cell clones (SPN0101, SPN0102, and SPN0103) and three control iPS cell clones are shown as mean ± SD. $^{**}P < 0.01$. (*F* and *G*) $CD34^+$ cells derived from SCN-iPS or control iPS cells were cultured in neutrophil differentiation medium (see text). On day 7, nonadherent cells were collected and analyzed. (*F*) Representative gel showing spliced (S) and unspliced (US) XBP-1 bands on day 7. (*G*) qRT-PCR analysis of the relative mRNA expression (target/HPRT expression) of BiP on day 7. Data are shown as mean ± SD. $^*P < 0.05$; different from control 1). (*H*) qRT-PCR analysis of the relative mRNA expression (target / HPRT expression) of C/EBP-α, C/EBP-β, C/EBP-ε, SPI1, and BCL2 genes in non-adherent cells derived from SCN-iPS cells (filled bars, SPN0103) and control iPS cells (open bars, control 1) on day 2 of suspension culture. Data are shown as the mean ± the s.d. ($^{**}P < 0.01$, $^*P < 0.05$).

iPS cell-derived myeloid cells might be caused by their apoptosis. In flow cytometric analysis, SCN-iPS cell-derived myeloid cells contained a significantly higher proportion of annexin V-positive cells than control iPS-derived myeloid cells on day 7 of culture, suggesting that the maturation arrest in myeloid cells derived from SCN-iPS cells might be caused by their apoptosis (Fig. 2*D*).

We next examined ELANE mRNA expression levels in nonadherent cells derived from SCN-iPS vs. control iPS cells (Fig. 2*E*). ELANE expression was significantly lower in nonadherent cells derived from SCN-iPS vs. control iPS cells on days 2 and 4 of culture ($P < 0.01$), as reported (16, 17). However, the former was a little higher than the latter on day 7 ($P < 0.01$). This result may be explained by the existence of SCN-iPS cell-derived myeloid cells arrested at an early stage along the neutrophil differentiation pathway even on day 7 of culture. We also examined the expression of proteinase 3 and azurocidin, which comprise a family of closely related genes encoding neutrophil granule proteins along with ELANE, and found these genes were more highly expressed on day 4 (Fig. S3).

It has been reported that induction of the endoplasmic reticulum stress (ER) response and the unfolded protein response (UPR) has been advanced as a potential explanation for the molecular pathogenesis of SCN (18, 19). Thus, we examined activation of the UPR by X-box binding protein 1 (XBP-1) mRNA splicing on day 7. As shown in Fig. 2*F*, SPN-iPS cells induced XBP-1 mRNA splicing. We also found the up-regulation of BiP

(also known as GRP78 or HSPA5) (Fig. 2*G*). These results suggested that ER stress response and UPR might be involved in the pathogenesis in SCN.

To examine further the differences in gene expression between the two cell types, a microarray analysis was carried out by using $CD34^+$ cells derived from SCN-iPS and control iPS cells (three clones of each) in suspension culture on day 2. At this early time point, differences in cell number and morphology were not yet readily discernible between SCN-iPS and control iPS cells, as shown in Fig. 2*A*. However, the microarray analysis revealed a differential expression of various genes between the two cell types. Transcription factor genes, which were related to neutrophil development [e.g., CCAAT/enhancer-binding protein (C/EBP)-α (20), C/EBP-β (21), C/EBP-ε (22), and SPI1 (also known as PU.1) (23)], were all down-regulated in SCN-iPS cells. B-cell chronic lymphocytic leukemia/lymphoma 2, which regulates cell death under ER stress through the core mitochondrial apoptosis pathway (24), was also down-regulated (Fig. 3*A*). These findings were confirmed by quantitative reverse-transcriptional PCR (qRT-PCR), as shown in Fig. 2*H*.

Notably, the down-regulation of the genes in SCN-iPS cells related to and regulated by the wingless-type mmtv integration site family, member 3a (Wnt3a)/β-catenin pathway [e.g., Wnt3a, lymphoid enhance-binding factor (LEF)-1, BIRC5 (also known as survivin), and cyclin D1] was also uncovered by microarray analysis and qRT-PCR (Fig. 3 *A*–*C* and Fig. S4). Therefore, we examined the effect of enhancement of Wnt3a/β-catenin signaling by exogenous Wnt3a addition on the neutrophil development of $CD34^+$ cells derived from SCN-iPS and control iPS cells. Although Wnt3a did not stimulate the survival, proliferation, and differentiation of $CD34^+$ cells derived from both iPS cells in the absence of cytokines stimulating myelopoiesis including G-CSF, the addition of Wnt3a to the neutrophil differentiation medium induced a dose-dependent increase in the percentage of mature neutrophils among the cultured cells, as shown in Fig. 3 *D* and *E*. Furthermore, when Wnt3a was added concurrently with 1,000ng/mL G-CSF, the proportion of mature neutrophils increased more than it did with Wnt3a or 1,000 ng/mL G-CSF alone, reaching a value comparable with that observed for control iPS cells (Fig. 4 *A* and *B*).

The reduced expression of LEF-1 (as regulated by the Wnt3a/β-catenin pathway) reportedly plays a critical role in the defective maturation of neutrophils in SCN patients (25). Therefore, we next examined LEF-1 mRNA expression in SCN-iPS–$CD34^+$ cells cultured in the presence of Wnt3a, G-CSF (1,000 ng/mL), or both. Wnt3a and G-CSF both enhanced LEF-1 mRNA expression, but the most significant increase was observed in the presence of Wnt3a plus G-CSF. LEF-1 expression in SCN-iPS–$CD34^+$ cells in response to Wnt3a plus G-CSF was almost the same as that in control iPS–$CD34^+$ cells (Fig. 4*C*). These results substantiate the importance of LEF-1 in neutrophil development and the pathogenesis of SCN, as shown (25). Moreover the

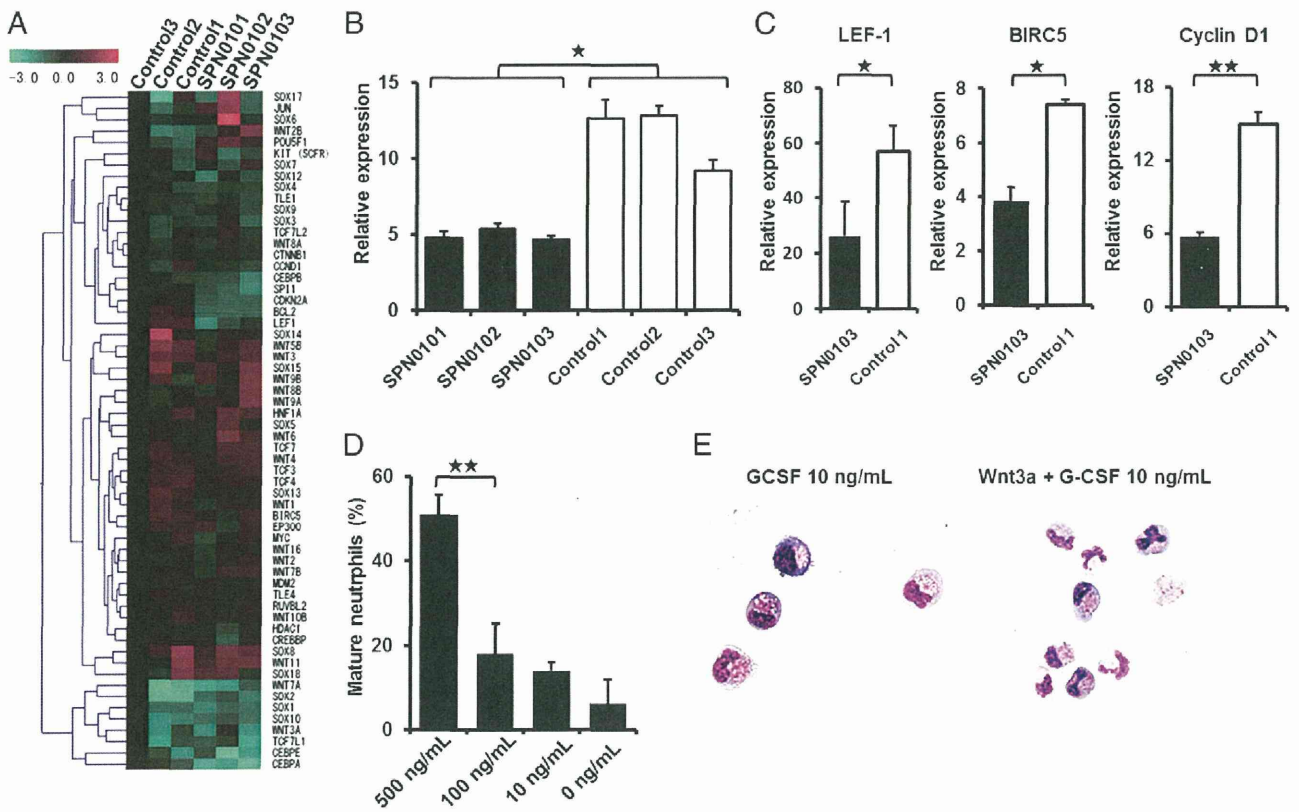

Fig. 3. Effects of Wnt3a on neutrophil development from SCN-iPS cells. (*A*) Heat map showing differential gene expression among SCN-iPS and control iPS cells on day 2. Red, high gene expression; blue, low gene expression compared with gene expression in control 3. (*B*) qRT-PCR analysis of the relative mRNA expression (target/HPRT expression) of Wnt3a on day 2. Filled and open bars indicate experiments using SCN-iPS cells (SPN0101, SPN0102, and SPN0103) and control iPS cells (controls 1, 2, and 3), respectively. Data are shown as mean ± SD. $^*P < 0.05$. (*C*) qRT-PCR analysis of the relative expression (target/HPRT expression) of genes regulated by the Wnt3a/β-catenin pathway (LEF-1, survivin, and cyclin D1) in SCN-iPS cells (filled bars, SPN0103) vs. control iPS cells (open bars, control 1) on day 2 of suspension culture. Data are shown as mean ± SD. $^{**}P < 0.01$; $^*P < 0.05$. (*D*) Proportion of mature neutrophils among the cells derived from SCN-iPS cells (SPN0102) on day 14 of suspension culture with dose escalation of Wnt3a. Data are shown as mean ± SD. $^{**}P < 0.01$. (*E*) Photographs of nonadherent cells on day 7 of suspension culture with or without Wnt3a (500 ng/mL) (400×; May–Grünwald–Giemsa staining).

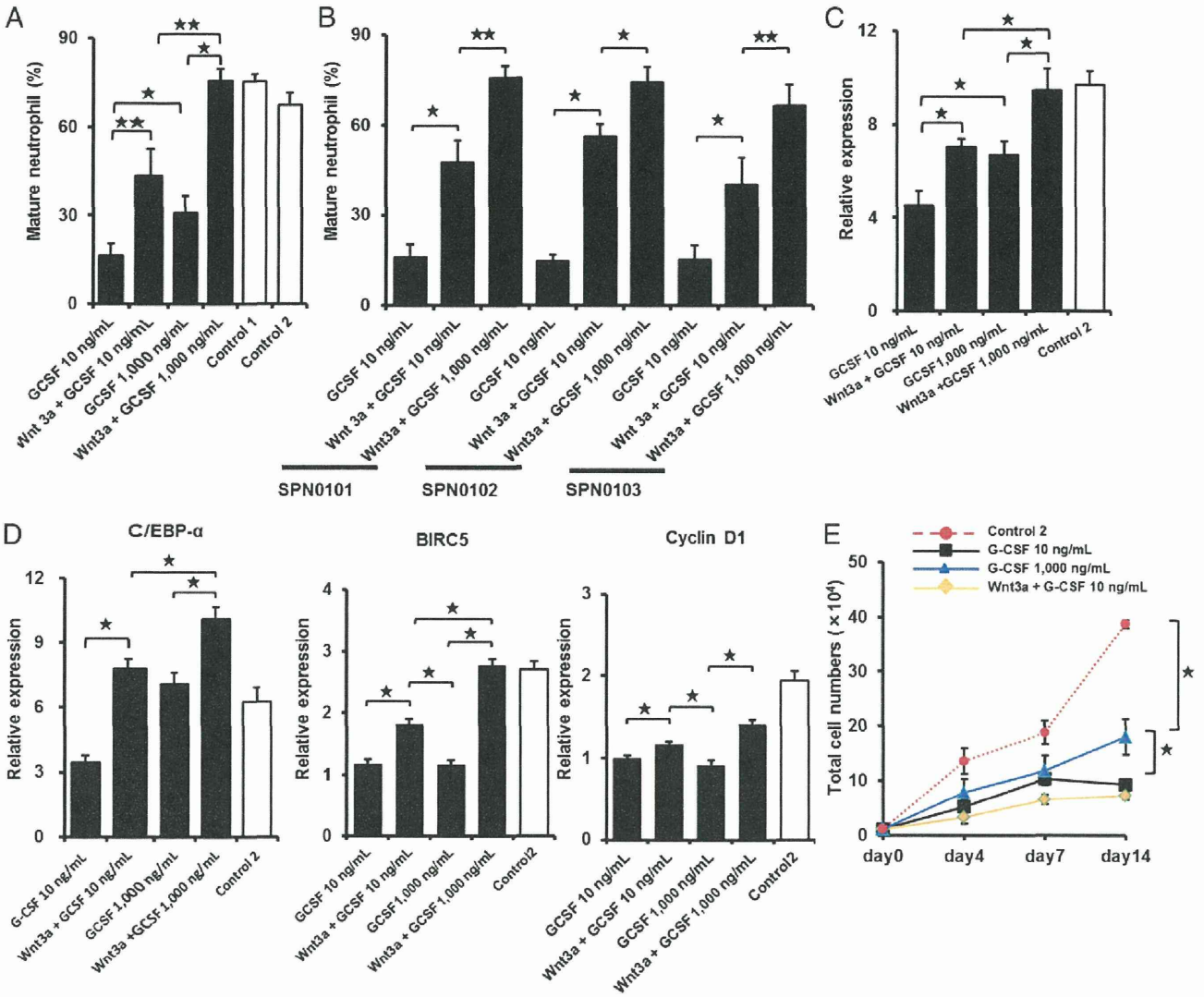

Fig. 4. Effects of Wnt3a in combination with high-dose G-CSF. (*A*) Filled and open bars show the proportion of mature neutrophils among the cells derived from SCN-iPS cells (SPN0101) on day 14 of suspension culture in the presence of neutrophil differentiation medium containing 10 ng/mL G-CSF (GCSF 10 ng/mL); 500 ng/mL Wnt3a and 10 ng/mL G-CSF (Wnt3a+GCSF 10 ng/mL); 1,000 ng/mL G-CSF (GCSF 1,000 ng/mL); or 500 ng/mL Wnt3a and 1,000 ng/mL G-CSF (Wnt3a + GCSF 1,000 ng/mL); and that from control iPS cells (controls 1 and 2) cultured in the neutrophil differentiation medium containing 10 ng/mL G-CSF, respectively. Data are shown as mean ± SD. $^{**}P < 0.01$; $^{*}P < 0.05$. (*B*) The proportion of mature neutrophils among the cells derived from three SCN-iPS cell clones (SPN0101, SPN0102, and SPN0103) on day 14 of suspension culture in the presence of neutrophil differentiation medium containing 10 ng/mL G-CSF (GCSF 10 ng/mL); 500 ng/mL Wnt3a and 10 ng/mL G-CSF (Wnt3a+GCSF 10 ng/mL); or 500 ng/mL Wnt3a and 1,000 ng/mL G-CSF (Wnt3a + GCSF 1,000 ng/mL). Data are shown as mean ± SD. $^{**}P < 0.01$; $^{*}P < 0.05$. (*C*) Filled and open bars show the relative expression (target/HPRT expression) of LEF-1 mRNA in SCN-iPS cells (SPN0101) on day 2 of suspension culture in the presence of differentiation medium containing the same combinations of Wnt3a and G-CSF as shown in *A* and that from control iPS cells (control 2), respectively. Data are shown as mean ± SD. $^{**}P < 0.01$; $^{*}P < 0.05$. (*D*) Filled and open bars show the relative expression (target/HPRT expression) of C/EBP-α, BIRC5, or cyclin D1 mRNA in SCN-iPS cells (SPN0101) on day 2 of suspension culture in the presence of differentiation medium containing the same combinations of Wnt3a and G-CSF as shown in *A* and that from control iPS cells (control 2), respectively. Data are shown as mean ± SD. $^{**}P < 0.01$; $^{*}P < 0.05$. (*E*) Total cell numbers of nonadherent cells in suspension cultures of 1×10^4 $CD34^+$ cells derived from control iPS cells (control 2; red broken line) and SCN-iPS cells (SPN0101) in the presence of neutrophil differentiation medium (black line) and those from SCN-iPS cells in the presence of neutrophil differentiation medium containing 500 ng/mL Wnt3a (yellow line) or 1,000 ng/mL G-CSF (black line). Data are shown as mean ± SD. $^{**}P < 0.05$.

administration of Wnt3a led to up-regulate C/EBP-α, cyclin D1, and BIRC5/survivin in addition to LEF-1 in the presence of G-CSF (Fig. 4*D*). These results suggested that the up-regulation of LEF-1 expression might promote granulopoiesis by increasing the expressions of cyclin D1, BIRC5/survivin, and C/EBP-α and its binding to LEF-1 in accordance with the previous report (25). Interestingly, Wnt3a did not stimulate the proliferation of myeloid cells, whereas 1,000 ng/mL G-CSF did to a certain extent (Fig. 4*E*). Hence, Wnt3a was capable of stimulating the maturation of impaired neutrophils in the presence of G-CSF, but not the proliferation of myeloid cells from SCN-iPS cells.

Importantly, aside from providing new insights into the mechanisms behind impaired neutrophil development in SCN patients, the present study demonstrates that agents activating the Wnt3a/β-catenin pathway are potential candidates for new drugs for SCN with mutations in the ELANE gene. Because endogenous G-CSF is readily increased in SCN patients (26), these activating agents may be viable alternatives to exogenous G-CSF treatment.

Materials and Methods

Additional information is available in *SI Materials and Methods*.

Generation of Human iPS Cells. BM fibroblasts from a patient with SCN and skin dermal fibroblasts from a healthy donor were acquired after obtaining informed consent after getting the approval by the Ethics Committee of the Institute of Medical Science, University of Tokyo, in accordance with the Declaration of Helsinki. The SCN patient presented with a heterozygous mutation in the ELANE gene in the 707 region of exon 5. SCN-iPS cells were established from the SCN-BM fibroblasts by transfection with the pMX retroviral vector, as described (10). This vector expressed the human transcription factors OCT3/4, SOX2, KLF4, and c-MYC. Control iPS cell clones, control 1 (TkDN4-M) and control 3 (201B7), were gifts from K. Eto and S. Yamanaka (Kyoto University, Kyoto), respectively (10, 11). Control 2 (SPH0101) was newly generated from another healthy donor's skin dermal fibroblasts by using the same methods.

Hematopoietic Colony Assay. A hematopoietic colony assay was performed in an aliquot of culture mixture, which contained 1.2% methylcellulose (Shin-Etsu Chemical), 30% (vol/vol) FBS, 1% (vol/vol) deionized fraction V BSA, 0.1 mM 2-mercaptoethanol (2-ME), α-minimum essential medium, and a cytokine mixture consisting of 100 ng/mL human stem cell factor (hSCF) (Wako), 100 ng/mL fusion protein 6 [FP6; a fusion protein of interleukin (IL)-6 and IL-6 receptor] (a gift from Tosoh), 10 ng/mL human IL-3 (hIL-3) (a gift from Kirin Brewery), 10 ng/mL human thrombopoietin (hTPO) (a gift from Kirin Brewery), 10 ng/mL human G-CSF (a gift from Chugai Pharmaceutical), and 5 U/mL human erythropoietin (a gift from Kirin Brewery). For dose escalation experiments, various concentrations (0, 1, 10, 100, and 1,000 ng/mL) of G-CSF were used instead of the cytokine mixture described above. Colony types were determined according to established criteria on day 14 of culture by in situ observations under an inverted microscope (IX70; Olympus) (27).

Suspension Culture and Neutrophil Differentiation Assay. $CD34^+$ cells (1×10^4 cells) were cocultured with irradiate confluent AGM-S3 cells in neutrophil differentiation medium containing Iscove's modified Dulbecco's medium, 10% FBS, 3 mM L-glutamine, 1×10^{-4} M 2-ME, 1×10^{-4} M nonessential amino acids solution, 100 ng/mL hSCF, 100 ng/mL FP6, 10 ng/mL hIL-3, 10 ng/mL hTPO, and 10 or 1,000 ng/mL human G-CSF. Wnt3a (10, 100, or 500 ng/mL) (R&D) was then added. The medium was replaced with an equivalent volume of fresh medium every 4 d. Living, nonadherent cells were counted following 0.4% trypan blue staining.

PCR primer. All primer sets used in this study are shown in Table S1.

Statistical Analysis. All data are presented as mean ± SD. $P < 0.05$ was considered significant. Statistical analyses were performed by using Prism software (GraphPad).

ACKNOWLEDGMENTS. We thank the individual with SCN who participated in this study; K. Eto for providing control iPS cells (control 1; TkDN4-M); S. Yamanaka for providing control iPS cells (control 3; 206B7); and E. Matsuzaka and S. Hanada for technical assistance. This work was supported by in part by Ministry of Education, Culture, Sports, Science, and Technology of Japan (MEXT) Grants-in-Aid (to Y.E.) and Project for Realization of Regenerative Medicine (MEXT) Grants-in-Aid (to K.Tsuji).

1. Zeidler C, Germeshausen M, Klein C, Welte K (2009) Clinical implications of *ELA2-, HAX1-*, and G-CSF-receptor (*CSF3R*) mutations in severe congenital neutropenia. *Br J Haematol* 144(4):459–467.
2. Freedman MH, et al. (2000) Myelodysplasia syndrome and acute myeloid leukemia in patients with congenital neutropenia receiving G-CSF therapy. *Blood* 96(2):429–436.
3. Dale DC, et al. (1993) A randomized controlled phase III trial of recombinant human granulocyte colony-stimulating factor (filgrastim) for treatment of severe chronic neutropenia. *Blood* 81(10):2496–2502.
4. Rosenberg PS, et al.; Severe Chronic Neutropenia International Registry (2006) The incidence of leukemia and mortality from sepsis in patients with severe congenital neutropenia receiving long-term G-CSF therapy. *Blood* 107(12):4628–4635.
5. Xia J, et al. (2009) Prevalence of mutations in ELANE, GFI1, HAX1, SBDS, WAS and G6PC3 in patients with severe congenital neutropenia. *Br J Haematol* 147(4):535–542.
6. Horwitz MS, et al. (2007) Neutrophil elastase in cyclic and severe congenital neutropenia. *Blood* 109(5):1817–1824.
7. Hajjar E, Broemstrup T, Kantari C, Witko-Sarsat V, Reuter N (2010) Structures of human proteinase 3 and neutrophil elastase—so similar yet so different. *FEBS J* 277(10): 2238–2254.
8. Fouret P, et al. (1989) Expression of the neutrophil elastase gene during human bone marrow cell differentiation. *J Exp Med* 169(3):833–845.
9. Pham CT (2006) Neutrophil serine proteases: Specific regulators of inflammation. *Nat Rev Immunol* 6(7):541–550.
10. Takayama N, et al. (2010) Transient activation of c-MYC expression is critical for efficient platelet generation from human induced pluripotent stem cells. *J Exp Med* 207(13):2817–2830.
11. Takahashi K, et al. (2007) Induction of pluripotent stem cells from adult human fibroblasts by defined factors. *Cell* 131(5):861–872.
12. Germeshausen M, Ballmaier M, Welte K (2007) Incidence of CSF3R mutations in severe congenital neutropenia and relevance for leukemogenesis: Results of a long-term survey. *Blood* 109(1):93–99.
13. Ma F, et al. (2007) Novel method for efficient production of multipotential hematopoietic progenitors from human embryonic stem cells. *Int J Hematol* 85(5):371–379.
14. Konishi N, et al. (1999) Defective proliferation of primitive myeloid progenitor cells in patients with severe congenital neutropenia. *Blood* 94(12):4077–4083.
15. Nakamura K, et al. (2000) Abnormalities of primitive myeloid progenitor cells expressing granulocyte colony-stimulating factor receptor in patients with severe congenital neutropenia. *Blood* 96(13):4366–4369.
16. Skokowa J, Fobiwe JP, Dan L, Thakur BK, Welte K (2009) Neutrophil elastase is severely down-regulated in severe congenital neutropenia independent of ELA2 or HAX1 mutations but dependent on LEF-1. *Blood* 114(14):3044–3051.
17. Kawaguchi H, et al. (2003) Dysregulation of transcriptions in primary granule constituents during myeloid proliferation and differentiation in patients with severe congenital neutropenia. *J Leukoc Biol* 73(2):225–234.
18. Köllner I, et al. (2006) Mutations in neutrophil elastase causing congenital neutropenia lead to cytoplasmic protein accumulation and induction of the unfolded protein response. *Blood* 108(2):493–500.
19. Grenda DS, et al. (2007) Mutations of the ELA2 gene found in patients with severe congenital neutropenia induce the unfolded protein response and cellular apoptosis. *Blood* 110(13):4179–4187.
20. Pabst T, et al. (2001) AML1-ETO downregulates the granulocytic differentiation factor C/EBPalpha in t(8;21) myeloid leukemia. *Nat Med* 7(4):444–451.
21. Hirai H, et al. (2006) C/EBPbeta is required for 'emergency' granulopoiesis. *Nat Immunol* 7(7):732–739.
22. Bedi R, Du J, Sharma AK, Gomes I, Ackerman SJ (2009) Human C/EBP-ε activator and repressor isoforms differentially reprogram myeloid lineage commitment and differentiation. *Blood* 113(2):317–327.
23. Friedman AD (2007) Transcriptional control of granulocyte and monocyte development. *Oncogene* 26(47):6816–6828.
24. Hetz C (2012) The unfolded protein response: Controlling cell fate decisions under ER stress and beyond. *Nat Rev Mol Cell Biol* 13(2):89–102.
25. Skokowa J, et al. (2006) LEF-1 is crucial for neutrophil granulocytopoiesis and its expression is severely reduced in congenital neutropenia. *Nat Med* 12(10):1191–1197.
26. Mempel K, Pietsch T, Menzel T, Zeidler C, Welte K (1991) Increased serum levels of granulocyte colony-stimulating factor in patients with severe congenital neutropenia. *Blood* 77(9):1919–1922.
27. Nakahata T, Ogawa M (1982) Hemopoietic colony-forming cells in umbilical cord blood with extensive capability to generate mono- and multipotential hemopoietic progenitors. *J Clin Invest* 70(6):1324–1328.

Supporting Information

Hiramoto et al. 10.1073/pnas.1217039110

SI Materials and Methods

Maintenance of Cells. Fibroblasts from a patient with SCN and a healthy donor were maintained in Dulbecco's modified Eagle medium (DMEM; Sigma) containing 10% FBS (HyClone). All human iPS cells were maintained on mitomycin C-treated (Wako) mouse embryonic fibroblast (MEF) feeder cells in human iPS cell maintenance medium [DMEM plus Ham's nutrient mixture F-12 (DMEM-F12; 1:1; Sigma) supplemented with 1×10^{-4} M 2-mercaptoethanol (2-ME; Wako), 2 mM L-glutamine (Invitrogen), 1% nonessential amino acids solution (NEAA; Invitrogen), 4 ng/mL human basic fibroblast growth factor (Wako), and 20% KNOCKOUT Serum Replacement (Invitrogen)]. The iPS cells were passaged weekly.

Immunohistochemistry. Immunohistochemical staining was performed as described (1). Briefly, human iPS cells were fixed with 4% (vol/vol) paraformaldehyde in phosphate buffer solution (PBS; Wako) at 4 °C for 30 min and permeabilized and blocked in 0.1% Triton X-100 (Nakalai-tesque) containing 5% (vol/vol) skim milk (Sigma) in D-PBS (Wako) for 30 min at 4 °C. The cells were first labeled with goat anti-human Nanog and goat anti-human Oct3/4 (1:50; R&D Systems) at 4 °C overnight and sequentially with anti-goat IgG (1:500; Invitrogen) for 30 min at room temperature. They were then observed by using a fluorescence microscope (IX70; Olympus).

Teratoma Formation and Histological Analysis. To produce teratomas, 1×10^6 iPS cells were inoculated into the testes of severe combined immunodeficiency mice (Central Institute for Experimental Animals). After 9–13 wk, the resected teratomas were fixed in 20% formalin and processed for paraffin sectioning. Teratomas were then stained with hematoxylin and eosin.

PCR. Total RNA was extracted by using an RNeasy Mini kit (Qiagen) as recommended by the manufacturer. Complementary DNAs were synthesized by using an iScript cDNA synthesis kit (Bio-Rad) as recommended by the manufacturer. Semiquantitative RT-PCR was performed with PrimeSTAR GXL DNA polymerase (Takara-bio) to determine the expression levels of genes of interest. qRT-PCR was performed by using SsoFast EvaGreen supermix (Bio-Rad). Genomic DNA was harvested by using the PureLink Genomic DNA kit (Invitrogen) as recommended by the manufacturer. Sequence PCR was performed as described (2). All RT-PCRs were performed on a C1000 thermal cycler (Bio-Rad), and all primer sets are shown in Table S1.

Microarray Analysis. Total RNA was extracted by using an RNeasy Micro kit (Qiagen), and RNA integrity was assessed by using a 2100 Bioanalyzer (Agilent Technologies). Aliquots (30 ng) of total RNA were amplified and labeled by using a Low Input Quick Amp Labeling Kit (Agilent Technologies) according to the manufacturer's instructions. Carbocyanin 3-labeled RNA (600 ng) was hybridized to a Whole Human Genome Oligonucleotide Microarray (Agilent Technologies), and the signals were detected by using a DNA microarray scanner (Agilent Technologies). The scanned images were extracted with Feature Extraction Software (Version 10.7.3.1; Agilent Technologies). Subsequent processing was performed by using the GenSpringGX11.5 software package (Agilent Technologies) and IPA 8.5 (Tomy Digital Biology). Significant difference in gene expression between SCN-iPS and control iPS cells in microarray analysis was determined by more than twofold change between the means of the two cell types.

Hematopoietic Cell Induction. To differentiate human iPS cells into hematopoietic cells, a coculture system with a murine stromal cell line, AGM-S3 (1), was used (3, 4). Briefly, 15-Gy-irradiated AGM-S3 cells were grown to confluence in each well of a six-well plate (Sumitomo Bakelite). Next, 50 undifferentiated human iPS cell colonies (each consisting of $\sim 1 \times 10^3$ cells) maintained on MEF feeder cells and individually selected were transferred onto each confluent AGM-S3 cell monolayer (containing $\sim 2 \times 10^5$ cells) and cultured in human iPS cell maintenance medium for 3 d. The culture medium was then changed to hematopoietic differentiation medium [Iscove's modified Dulbecco's medium (IMDM) containing 10% FBS, 3 mM L-glutamine, 5.5 mg/mL human transferrin, 50 ng/mL ascorbic acid, 1×10^{-4} M 2-ME, 1×10^{-4} M NEAA, and 10 ng/mL human vascular endothelial growth factor] and was replaced every day. Twelve days later, cobblestone regions and iPS-derived cells with a proliferative morphology emerged. At this time, the cocultured cells were harvested, and $CD34^+$ cells were separated by using a Dynal CD34 Progenitor Cell Selection System (Invitrogen).

Staining. For May–Grünwald–Giemsa staining, 5×10^3 cells were stained with May–Grünwald solution for 3 min and Giemsa solution for 20 min. Samples were observed by using a light microscope (BX50; Olympus).

XBP-1 Splicing Assay. XBP-1 mRNA processing was measured by using a described assay (5). In brief, we harvested nonadherent cells at day 7 in suspension culture of neutrophil differentiation and obtained total RNA using an RNeasy Micro kit. Complementary DNAs were synthesized by using an iScript cDNA synthesis kit according to the manufacturer' instructions. Then, we amplified the XBP-1 cDNA by RT-PCR, and the PCR product was digested with PstI restriction enzyme (New England Biolabs) and resolved on a 2% agarose gel (Wako).

Apoptosis Assay. SCN-iPS and control iPS–$CD34^+$ cells (1×10^4 cells each) were cocultured in suspension with AGM-S3 cells in neutrophil differentiation medium. At day 7, apoptotic cells were analyzed by flow cytometry using an annexin V-FITC Apoptosis Detectin Kit (Medical and Biological Laboratories) according to the manufacturer' instructions.

1. Ma F, et al. (2012) Differentiation of human embryonic and induced pluripotent stem cells in coculture with murine stromal cells. *Springer Protocols*, eds Ye K, Jin S (Springer, Secaucus, NJ), pp 321–335.
2. Germeshausen M, Ballmaier M, Welte K (2007) Incidence of CSF3R mutations in severe congenital neutropenia and relevance for leukemogenesis: Results of a long-term survey. *Blood* 109(1):93–99.
3. Ma F, et al. (2007) Novel method for efficient production of multipotential hematopoietic progenitors from human embryonic stem cells. *Int J Hematol* 85(5): 371–379.
4. Ma F, et al. (2008) Generation of functional erythrocytes from human embryonic stem cell-derived definitive hematopoiesis. *Proc Natl Acad Sci USA* 105(35):13087–13092.
5. Calfon M, et al. (2002) IRE1 couples endoplasmic reticulum load to secretory capacity by processing the XBP-1 mRNA. *Nature* 415(6867):92–96.

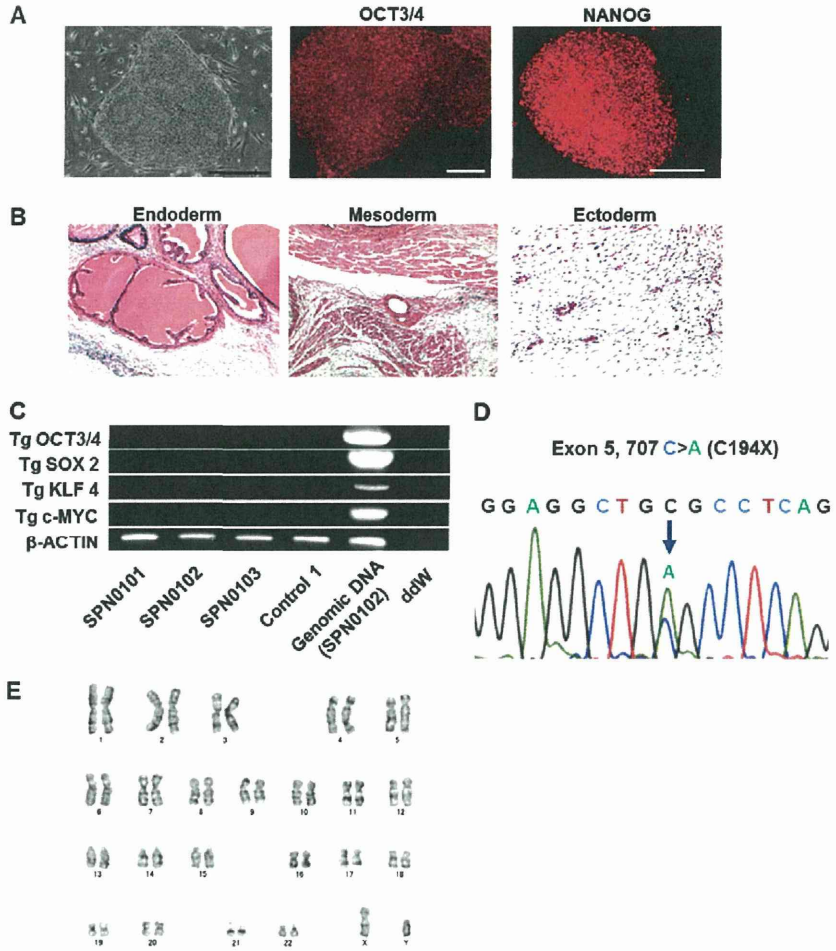

Fig. S1. Generation of SCN-iPS cells from an SCN patient with a heterologous ELANE gene mutation. (*A*) Morphology and expression of pluripotent stem cell markers (NANOG and OCT3/4) in SCN-iPS cells (SPN0101). (Scale bars, 200 μm.) (*B*) Hematoxylin and eosin staining of teratomas derived from SCN-iPS cells (SPN0101). The teratomas were composed of various types of tissues, including glandula thyreoidea (endoderm, 100×), muscle (mesoderm, 100×), and neural (ectoderm, 200×) tissues. (*C*) The silencing of transgenic (Tg) gene expression derived from retrovirus vector-expressed human OCT3/4, human SOX2, human KLF-4, and human c-MYC. (*D*) A mutation in the ELANE gene (exon 5, 707 region C > A; C194X mutation) was detected in SCN-iPS cells (SPN0101); this mutation was identical to that present in the donor patient. The same mutation was detected in all three SCN-iPS cell clones. (*E*) Representative karyotype of SCN-iPS cells (SPN0101) showing 46,XY.

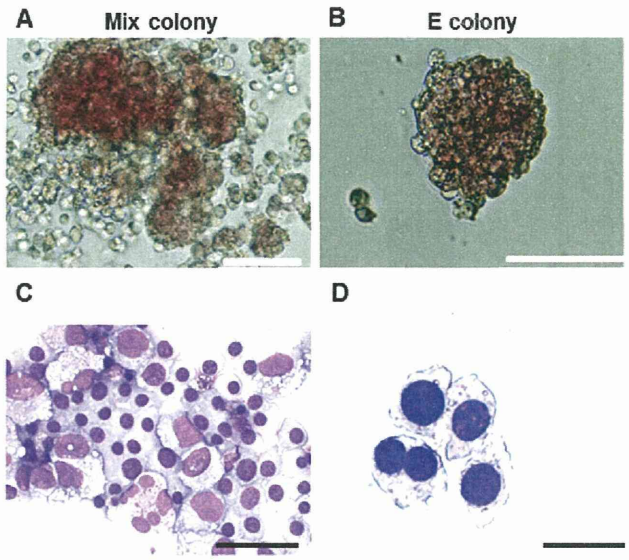

Fig. S2. Photographs of hematopoietic colonies derived from SCN-iPS cells in the presence of a cytokine mixture. (*A* and *C*) A mixed-lineage (Mix) colony derived from SCN-iPS cells (SPN0102) (*A*) and its constituent cells (*C*). (*B* and *D*) An erythroid (E) colony (*B*) and its constituent cells (*D*). (Scale bars: *A*, 80 μm; *B*, 20 μm; *C* and *D*, 50 μm.)

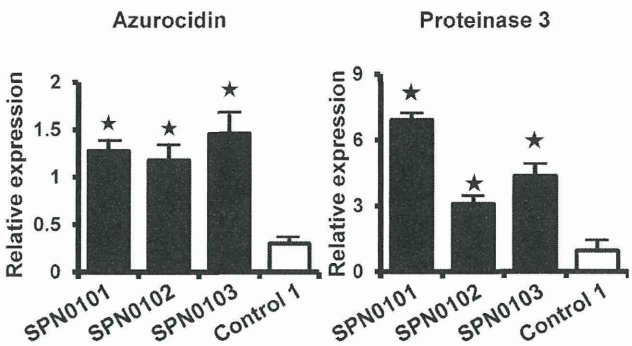

Fig. S3. qRT-PCR analysis of azurocidin and proteinase 3 in CD34+ cells derived from SCN-iPS and control iPS cells. $CD34^+$ cells derived from SCN-iPS or control iPS cells were cultured in neutrophil differentiation medium (see text). On day 4, nonadherent cells were collected and analyzed. Filled and open bars show the relative expression (target/HPRT expression) of azurocidin and proteinase 3 mRNA in three SCN-iPS cells (filled bars) and a control iPS cell (control 1; open bar). Data are shown as mean ± SD. $^*P < 0.05$.

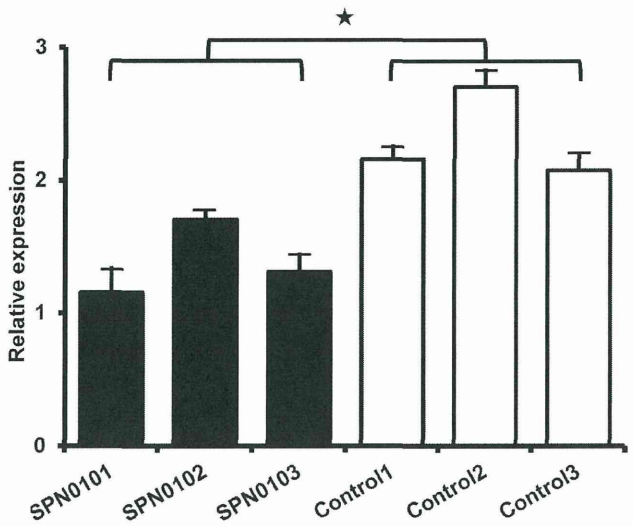

Fig. S4. qRT-PCR analysis of BIRC5/survivin expression in $CD34^+$ cells derived from SCN-iPS and control iPS cells. $CD34^+$ cells derived from SCN-iPS or control iPS cells were cultured in neutrophil differentiation medium (see text). On day 2, nonadherent cells were collected and analyzed. Filled and open bars show the relative expression (BIRC5/HPRT expression) in three SCN-iPS and control iPS cells, respectively. Data are shown as mean ± SD. $^\star P < 0.05$.

Table S1. Primers used for analyzing iPS cells and hematopoiesis

Cells	Primer
Reprogramming factors (semiquantitative RT-PCR)	
Tg Forward	
pMXs-AS3266	5′-TACAGGTGGGGTCTTTCATTC-3′
Tg OCT3/4	
Oct3/4-S880	5′-CAACGAGAGGATTTTGAGGCT-3′
Tg SOX2	
hSOX2-S614	5′-TGCAGTACAACTCCATGACCA-3′
Tg KLF4	
hKLF4-S1180	5′-TGCGGCAAAACCTACACAAAG-3′
Tg c-MYC	
hMyc-S1001	5′-GACAGATCAGCAACAACCGAA-3′
B-ACTIN	
rhb-actin-S	5′-GCAGGAGATGGCCACGGCGGC-3′
rhb-actin-AS	5′-TCTCCTTCTGCATCCTGTCGGC-3′
Hematopoiesis analysis (qRT-PCR)	
ELANE	
ELANE qPCR FW	5′-GCTACCATCAACGCCAACGTG-3′
ELANE qPCR RV	5′-GCTGGGTGAGGGTCGGTTTGTGC-3′
Azurocidin	
AZU1 qPCR FW	5′-CTGCTGATGGAAAACGTCTG-3′
AZU1 qPCR RV	5′-CAGCTGCTTCCAAAGCCA-3′
Proteinase 3	
PRTN3 qPCR FW	5′-GTGGATCAAGGTGCCTCC-3′
PRTN3 qPCR RV	5′-GTGCTGCTGGCCTTGCT-3′
BIP	
HSPA5 qPCR FW	5′-TGTCTTTTGTCAGGGGTCTTT-3′
HSPA5 qPCR RV	5′-CACAGTGGTGCCTACCAAGA-3′
C/EBP-α	
C/EBP-α qPCR FW	5′-TGGACAAGAACAGCAACGAG-3′
C/EBP-α qPCR RV	5′-TTGTCACTGGTCAGCTCCAG-3′
C/EBP-β	
C/EBP-β qPCR FW	5′-GCGCGAGCGCAACAACA-3′
C/EBP-β qPCR RV	5′-TGCTTGAACAAGTTCCGCAG-3′
C/EBP-ε	
C/EBP-ε qPCR FW	5′-GACCTACTATGAGTGCGAGCCT-3′
C/EBP-ε qPCR RV	5′-ACACCCTTGATGAGGGTAGCAG-3′
PU.1	
PU.1 qPCR FW	5′-GAGAGCCATAGCGACCATTACT-3′
PU.1 qPCR RV	5′-GTACAGGCGGATCTTCTTCTTG-3′
BCL2	
BCL2 qPCR FW	5′-TGGGATGCCTTTGTGGAACT-3′
BCL2 qPCR RV	5′-GAGACAGCCAGGAGAAATCAAAC-3′
LEF-1	
LEF-1 qPCR FW	5′-GACGAGATGATCCCCTTCAA-3′
LEF-1 qPCR RV	5′-AGGGCTCCTGAGAGGTTTGT-3′
Cyclin D1	
Cyclin D1 qPCR FW	5′-AGGTCTGCGAGGAACAGAAGTG-3′
Cyclin D1 qPCR RV	5′-TGCAGGCGGCTCTTTTTC-3′
BIRC5	
Survivin qPCR FW	5′-ACCACCGCATCTCTAC-3′
Survivin qPCR RV	5′-TCCTCTATGGGGTCGT-3′
Wnt3a	
Wnt3a qPCR FW	5′-ATGAGCGTGTCACTGCAAAG-3′
Wnt3a qPCR RV	5′-ACAGCCTGGCCATCTTCG-3′
HPRT	
HPRT-S	5′-TGACCTTGATTTATTTTGCATACC-3′
HPRT-AS	5′-CGAGCAAGACGTTCAGTCCT-3′
Sequence PCR	
ELANE	
long-ex2F (PCR)	5′-GATCCCGTGGGTTCCTGG-3′
long-ex3R (PCR)	5′-TCAACGGCCCATGGCGGGTAT-3′
sEq. 2F (Sequence)	5′-AGAGGCCCCGTGGCCGG-3′
sEq. 3F (Sequence)	5′-AGCACCTTCGCCCTCAGG-3′